Molecular Motion in Phenpropylammonium Chloride Studied by Deuterium NMR

Marco L. H. Gruwel* and Roderick E. Wasylishen

Department of Chemistry, Dalhousie University, Halifax, NS, Canada B3H 4J3

Z. Naturforsch. **47a**, 1073–1086 (1992); received February 19, 1992

Cation dynamics in phenpropylammonium chloride, $C_6H_5(CH_2)_3NH_3^+Cl^-$, were studied in three different solid phases by means of ^2H nmr. Both ^2H nmr line shapes and spin-lattice relaxation studies were performed on the ammonium head group, the adjacent methylene group and the phenyl-ring. In the low temperature phase, solid III, the $-ND_3$ group dynamics were dominated by C_3 jumps about the C–N axis. From the observed minima in T_{1Z} and T_{1Q} a quadrupole coupling constant of 165 ± 5 kHz was obtained. The ^2H nmr line shapes of the methylene group indicate that this group does not execute any large amplitude motion in the low temperature phase. In contrast, the phenyl ring deuterium nuclei give rise to line shapes characteristic of C_2 ring flips about the $C_{para}-C_{ipso}$ axis.

In the solid II phase the ^2H nmr line shapes of both the $-ND_3$ and $-CD_2-$ groups are characterized by asymmetric Pake powder patterns. Since one of the principal components of the electric field gradient tensor remains temperature independent for both groups, it was concluded that these groups perform planar large-amplitude motions between two sites.

Axially symmetric spectra were obtained for all three groups in the high temperature phase, solid I. The ^2H nmr line shapes indicate the presence of whole ion reorientation about a molecular axis. In addition, the $-ND_3$ groups perform C_3 jumps about the C–N axis and the $-C_6D_5$ group display line shapes characteristic for rotational diffusion about the $C_{para}-C_{ipso}$ axis.

I. Introduction

A combination of deuterium (^2H) nmr line shape and relaxation rate studies has been used to obtain a description of the reorientational dynamics of the hydrochloride salt of phenpropylamine. Phenpropylammonium chloride, $C_6H_5CH_2CH_2CH_2NH_3^+Cl^-$, will be conveniently abbreviated to PPNCl. The crystal structure of PPNCl has, to the knowledge of the authors, not been reported in the literature. However, the crystal structure of phenethylammonium chloride is known at room temperature [1]. Recently Knop et al. [2] determined phenethylammonium bromide to be isostructural with its chloride analogue at room temperature. These phenethylammonium compounds form a chain structure which has a bilayer type of symmetry [1, 2]. The crystals consist of a sawtooth layer of halide ions which are hydrogen bonded with the ammonium head groups in such a way that the phenalkyl residue remains perpendicular to the long axis of the sawtooth layer. The ammonium head group forms strong, nearly linear, hydrogen bonds with the three neighbouring halide ions [1]. It is interesting to note that the x-ray coefficients of thermal motion at room temperature increase in the order: Cl, N, C (alkyl chain), C (phenyl ring).

Recently the phase transitions in the phenethyl- and phenpropyl-ammonium halides have been identified using differential scanning calorimetry (DSC) [3]. Although reasonably accurate transition temperatures and enthalpy changes can be obtained from such measurements, it is difficult to deduce microscopic and/or dynamic information using DSC. For PPNCl the temperatures and entropy change associated with these transitions are listed in Table 1. In order to characterize the molecular dynamics taking place in these solid phases, ^2H nmr line shape and relaxation rate studies of Zeeman and quadrupolar order were carried out as a function of temperature. Using specifically labelled deuterated analogues, the reorientational motion of the ammonium headgroup, the alkyl-chain and the phenyl-ring have been independently studied and characterized. In a previous publication [4] we demonstrated the dynamical information available from a detailed ^2H nmr study of the related salt, phenethylammonium bromide.

* Present address: Physiologisches Institut I, Medizinische Einrichtungen, Heinrich-Heine-Universität, Moorenstr. 5, W-4000 Düsseldorf 1, Germany.

Reprint requests to Professor R. E. Wasylishen, Department of Chemistry, Dalhousie University, Halifax, Nova Scotia, Canada, B3H 4J3.

0932-0784 / 92 / 1000-1073 $ 01.30/0. – Please order a reprint rather than making your own copy.

Table 1. Solid–solid phase transitions in PPNCl from DSC measurements [3].

Phase	Transition [K]	ΔS [R]
III	343	2.18
II	368	1.39
I	452 (d)	

(d) = decomposition temperature.

II. Theory

i) Line Shapes

Frequency spectra of deuterium spins are dominated by the quadrupole interaction which is taken as a first order perturbation to the Zeeman interaction [5]. Under these conditions the nmr frequency is given by

$$\omega = \omega_0 \pm (3/2)\pi \langle \chi^2 \rangle^{1/2} \cdot [(3\cos^2\theta - 1)/2 - \eta(\sin^2\theta \cos 2\phi)/2], \quad (1)$$

where χ is the nuclear quadrupole coupling constant (QCC) in Hz, ω_0 is the Larmor frequency and η is the electric field gradient (efg) asymmetry parameter in the X–^{2}H bond. The orientation of the efg principal axis frame with respect to the static magnetic field is given by angles (θ, ϕ). The asymmetry of the efg tensor will be assumed to be negligible for the C–^{2}H and N–^{2}H bonds studied [6]. Deuterium nmr powder spectra typically have a maximum width of about 500 kHz. Anisotropic motion will lead to partially narrowed spectra with specific line shapes depending on the type and time scale of the motion. When the rate of the molecular motion is of the same order as the QCC, one can observe prominent line shape changes [6]. This region in time is often referred to as the intermediate exchange region.

Due to the dead time of the receiver a direct detection of the full free induction decay (FID), after a $\pi/2$ pulse, is not possible. However, one can obtain a solid echo spectrum [7] which is the Fourier transform of the FID generated by two $\pi/2$ pulses, phase shifted by $\pi/2$ and separated by a time τ_1 [8, 9]. For motional correlation times less than 10^{-8} s or greater than 10^{-3} s the line shape generated by the echo sequence becomes independent of τ_1 and the correlation time, τ. Thus, in these cases, the solid echo and the true line shape spectra are essentially identical. For correlation times in the intermediate exchange region the intensity and line shape of the solid echo can substantially differ from the true spectrum [10–12].

For any type of motion of the ^{2}H efg tensor with respect to the laboratory frame, the expression for the resonance frequency, ω, becomes different from that given in (1). In these case of an axially symmetric efg ($\eta = 0$), the $(3\cos^2\theta - 1)/2$ term in (1) has to be replaced by [13]

$$(1/4)(3\cos^2\beta - 1)(3\cos^2\theta_1 - 1) + (3/4)[\sin 2\beta \sin 2\theta_1 \cos(\gamma + \phi + \delta) + \sin^2\beta \sin^2\theta_1 \cos 2(\gamma + \phi + \delta)]. \quad (2)$$

Here the reorientation axis is defined by the Euler angles (α, β, γ) with respect to the efg principal axes frame. The angle δ represents the jump angle and (θ_1, ϕ) are Euler angles describing the orientation of the molecular frame with respect to the laboratory frame. Molecular motion will now introduce averaging over the angles (θ_1, ϕ). When the rate of molecular motion is greater than the QCC and is about an axis of threefold or higher symmetry, the effective motional induced spectral asymmetry is zero (*vide infra*). Even if the efg tensor has non zero efg asymmetry in the principal axes frame, motion with threefold or higher symmetry will result in an axially symmetric line shape.

For two site exchange processes such as C_2 jumps, spectral asymmetry will be introduced into the powder line shape by the motion [11, 14–18]. In Fig. 1 the effect of C_2 flips in the intermediate exchange region on the ^{2}H nmr line shape is shown. A small change in the jump rate results in a large change in the Fourier transform of the solid echo. For the example in Fig. 1, orientations of the static magnetic field and the largest component of the C–^{2}H efg tensor of $\pi/2$ or $\pi/3$ are not affected by the jumps. These orientations will thus appear with a relatively long spin-spin relaxation time compared to the other possible angles. As a result, the $\pi/2$ and $\pi/3$ orientations will appear with a large signal amplitude in the powder line shape since that of the others will vanish during the echo formation due to the short spin-spin relaxation time. Note that the intensity of the line shapes shown in Fig. 1 have been scaled up in order to show the typical features of the line shapes. The total line shape intensity could drop to about 5–10% of the fast or slow motion limit line shape.

ii) Relaxation

In this section the effects of pure C_3 jumps on the spin-lattice relaxation of the ^{2}H magnetization of

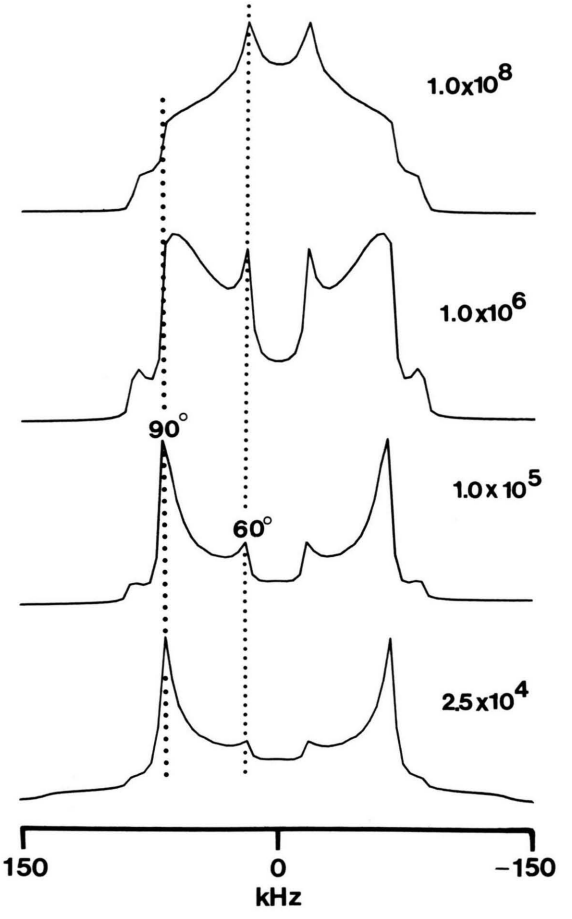

Fig. 1. Line shape simulations for off-axis deuterons in a phenyl ring performing C_2 jumps. The jump rates are given next to each line shape. Each spectrum was simulated with an echo delay of 40 μs.

Table 2. Goniometric coefficients for the spectral densities of the pure C_3 flip motion.

$A_1 = \sin^2 2\Theta$	$B_3 = \sin^3\theta\cos\theta$
$A_2 = \sin^4\Theta$	$B_4 = \cos^2\theta + \cos^2 2\theta$
$A_3 = \sin^3\Theta\cos\Theta$	$B_5 = \sin^2\theta + (1/4)\sin^2 2\theta$
	$B_6 = 1 + 6\cos^2\theta + \cos^4\theta$

$-ND_3$ groups will be discussed. The model employed here is due to Torchia and Szabo [19]. For quadrupole interactions, Spiess [20] derived general expressions for the spin-lattice relaxation rate of Zeeman and quadrupolar order:

$$R_{1Z} = (3/4)\pi^2 \langle\chi^2\rangle [J_1(\omega_0) + 4J_2(2\omega_0)],$$
$$R_{1Q} = (3/4)\pi^2 \langle\chi^2\rangle [3J_1(\omega_0)]. \quad (3)$$

The spectral densities, $J_m(m\omega)$, are the cosine transform of the efg time autocorrelation functions. Here we will use the spectral densities for pure C_3 jumps as obtained by Torchia and Szabo [19]:

$$J_1(\omega_0) = (3/8)[A_1 B_4 + A_2 B_5 - 8A_3 B_3 \cos 3\phi]\, g(\omega_0, \tau),$$
$$J_2(2\omega_0) = (3/32)[4A_1 B_5 + A_2 B_6 + 8A_3 B_3 \cos 3\phi]\, g(2\omega_0, \tau), \quad (4)$$

where

$$g(m\omega_0, \tau) = \frac{\tau}{1 + (m\omega_0\tau)}.$$

The jump correlation time τ is defined as $1/(3k)$, where k is the jump rate. The correlation time is assumed to be thermally activated, such that

$$\tau = \tau_\infty \exp(E_a/RT), \quad (5)$$

where E_a is the activation energy for the C_3 jumps and τ_∞ is the correlation time at infinite temperature. The coefficients A_i and B_i are listed in Table 2. All the coefficients A_i are determined by molecular geometry. In the discussion that follows it will be assumed that the angle Θ between the C_3 jump axis and the $N-{}^2H$ bond will be 70.5°. The coefficients B_i introduce the orientation dependence in the relaxation rate of Zeeman and quadrupolar order. Note that the ^2H nmr line shape can be fully described by an axially symmetric powder pattern, i.e., there is no ϕ dependence obtained from the static line shape, this follows from the addition theorem of spherical harmonics. On the other hand, the relaxation of the ^2H magnetization depends on both Θ and ϕ due to the presence of off-diagonal elements in the C_3 jump matrix [19]. This can be understood in terms of the properties of second rank spherical harmonics. These functions form the lattice part of the spin Hamiltonian [5]: $H \triangleq Y_{2,m}(\theta, \phi) \triangleq e^{im\phi}$. Deuterium line shapes are thus independent of ϕ for motion with 3-fold or higher symmetry since $|m| = 2$ is the maximum value obtained by $Y_{2,m}(\theta, \phi)$. However, for nuclear magnetic relaxation, the product of $Y_{2,m}(\theta, \phi)$ with its complex conjugate has to be considered. Using the addition theorem of angular momentum, this product can be shown to contain $Y_{4,m}(\theta, \phi)$. Thus a maximum value of $|m| = 4$ in relaxation processes can occur. Reorientation processes with 5-fold or higher symmetry will thus only exhibit diagonal elements in the jump matrix [19]. This angular dependence causes non-exponential relaxation

within the powder pattern. However the ϕ dependence in the spectral density vanishes for $\theta = 0°$ or 90°, enabling one, in principle, to measure exponential relaxation of these frequency sites. Only for the relaxation of Zeeman order in the extreme narrowing limit, $\omega_0 \tau \ll 1$, will this ϕ dependence also disappear. A complication of the interpretation of the relaxation rate of the "$\theta = 90°$" orientation in a Pake powder pattern arises from the fact that a ^2H nmr powder pattern consists of a superposition of two transition frequency distributions as given by (1). This results in an actual overlap of the $\theta = 90°$ and $\theta = 35.3°$ orientations each belonging to a different transition within the three-level system. The amplitude ratios of the transitions at these orientations is 1:0.58 for the $\theta = 90°$ and $\theta = 35.3°$ orientations respectively [21]. The explicit expression for the relaxation rate of the "$\theta = 90°$" orientation thus is

$$R_1^{\mathrm{Obs}}(\text{“}\theta = 90°\text{”}) = (1/1.58)\,[R_1(\theta = 90°) + 0.58\,R_1(\theta = 35.3°)]\,. \quad (6)$$

Equation (6) shows that the "$\theta = 90°$" orientation in a Pake doublet still contains a ϕ dependence in the relaxation rate. Since this dependence is difficult to measure [19], a powder average of these ϕ terms was calculated. Using $\Theta = 70.5°$, assuming a tetrahedral configuration for $-ND_3$, the spectral densities for the different powder orientations were calculated and are listed in Table 3. The ratio of the Zeeman and quadrupolar order spin-lattice relaxation rate for the "$\theta = 90°$" and $\theta = 0°$ orientations in the powder pattern is

$$\frac{R_{1Z}^{\mathrm{Obs}}(\text{“}\theta = 90°\text{”})}{R_{1Q}^{\mathrm{Obs}}(\text{“}\theta = 90°\text{”})} = (1/3)\left[0.733 + 1.465\,\frac{g(2\omega_0, \tau)}{g(\omega_0, \tau)} + 0.267 + 1.857\,\frac{g(2\omega_0, \tau)}{g(\omega_0, \tau)}\right], \quad (7a)$$

$$\frac{R_{1Z}(\theta = 0°)}{R_{1Q}(\theta = 0°)} = (1/3)\left[1 + 8\,\frac{g(2\omega_0, \tau)}{g(\omega_0, \tau)}\right], \quad (7b)$$

Table 4 summarizes the slow and fast motion limits of (7a, b). It is clear from this table that the inclusion of the $\theta = 35.3°$ orientation in the calculations is important.

In Fig. 2 the Zeeman and quadrupolar relaxation times are shown as a function of the C_3 jump correlation time. The calculations were performed using (3), (4), and (6).

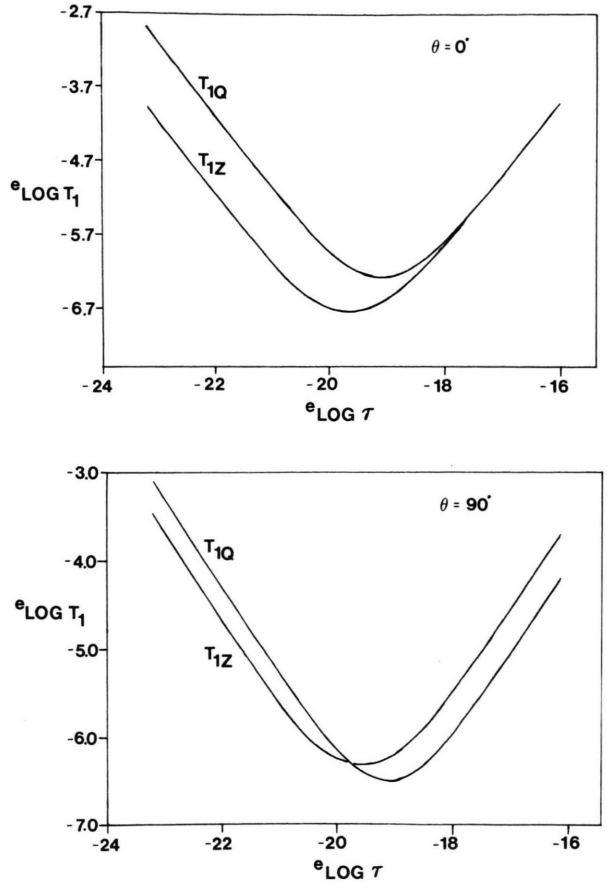

Fig. 2. ^2H Zeeman- and quadrupole spin-lattice relaxation times for pure C_3 flips as a function of the jump time ($= 1/(3k)$). For the calculations a QCC of 174 kHz and a η value of 0 was used.

Table 3. Spectral densities of the C_3 flip motion at specific orientations of the ^2H bond with respect to the external field.

Orientation	Spectral density
$\theta = 90°$	$J_1(\omega_0) = (12/27)\,g(\omega_0, \tau)$ $J_2(2\omega_0) = (6/27)\,g(2\omega_0, \tau)$
$\theta = 35.3°$	$J_1(\omega_0) = (4/27)\,(17/9)\,g(\omega_0, \tau)$ $J_2(2\omega_0) = (2/27)\,(59/9)\,g(2\omega_0, \tau)$
$\theta = 0°$	$J_1(\omega_0) = (8/27)\,g(\omega_0, \tau)$ $J_2(2\omega_0) = (16/27)\,g(2\omega_0, \tau)$

Table 4. Ratios of Zeeman- and quadrupolar spin-lattice relaxation rates for the $\theta = 0°$ and "$\theta = 90°$" orientations.

$R_{1Z}(\theta)/R_{1Q}(\theta)$	$\omega_0 \tau \ll 1$	$\omega_0 \tau \gg 1$
"$\theta = 90°$	1.44 (1)	0.610 (0.5)
$\theta = 0°$	3.00	1.00

The numbers in parentheses are obtained if one excludes the contribution of the $\theta = 35.3°$ orientation in the calculations.

III. Experimental

All ^2H nmr experiments were performed on a Bruker MSL 200 at 30.72 MHz. Typical $\pi/2$ pulse lengths were 4.0–4.5 μs. The ^2H nmr line shapes were acquired with a solid echo pulse sequence [7, 22] which consists of two $\pi/2$ pulses phase shifted by $\pi/2$:

$$\pi/2|_x \cdots \tau_1 \cdots \pi/2|_y \cdots \tau_2 \cdots \text{ACQ}\,.$$

Typical τ_1 and τ_2 values were 40 μs. All echoes were acquired with the transmitter positioned at the centre of the line shape. A sweep width of 500 kHz was used throughout all the experiments. Since the obtained spectra were symmetric, folding about the centre frequency was applied to increase the signal to noise ratio.

Zeeman spin-lattice relaxation experiments were performed using the solid echo sequence after the application of an inversion, π, pulse [23]. After the inversion pulse a variable time delay was included to observe relaxation. The spectra in a relaxation rate experiment were not folded. All relaxation rates were obtained from peak heights obtained at eight or more relaxation delays. Relaxation rates of quadrupolar order (R_{1Q}) were obtained using a modified Jeener-Broekaert pulse sequence [24, 25]:

$$\pi/2|_y \cdots \tau_1 \cdots \pi/4|_x \cdots t \cdots \pi/4|_x \cdots \tau_2 \cdots \cdots \pi/2|_x \cdots \tau_3 \cdots \text{ACQ}\,.$$

In this pulse sequence the time delay t serves as a relaxation delay for the created quadrupolar order. The delays τ_2 and τ_3 serve the same purpose as τ_1 and τ_2 in the solid echo sequence since the last pulse in the modified Jeener-Broekaert pulse sequence refocusses the Jeener echo. The value of τ_1 was determined from the solid echo line shape [25].

For temperatures above room temperature, the temperature in the nmr probe was controlled with air and a heater built into the probe. Low temperatures were attained and controlled with cooled nitrogen gas and the heater in the probe. The temperature was stable within 1 K after reaching equilibrium. The thermocouple used was calibrated outside the probe at three different temperatures between 77 and 373 K. Both the sample and the thermocouple were placed within a glass dewar, 1.5 cm apart.

Most deuterated compounds were prepared by M. van Oort [26]. Specific deuteration was carried out at three positions: the phenyl-ring (all positions), the alkyl-chain (the methylene group adjacent to the ammonium head group only) and the ammonium head group. Before use, the degree of deuteration of the samples was checked by means of solution ^{13}C nmr. Finally the samples were degassed and sealed under vacuum in thin walled glass tubes of approximately 2.5 cm length and 1.0 cm diameter.

All spectral simulations were performed with a Fortran computer program which was obtained from Dr. R. G. Griffin, Dr. R. J. Wittebort [10b] and an updated version from R. Weber. The program was run on the Dalhousie University VAX 8800 mainframe computer. With the exception of the T_{1Z} simulations, the simulated solid echo spectra were not corrected for finite pulse length distortions [27].

IV. Results and Discussion

i) Reorientational Symmetry of the $-ND_3$ Group Obtained from ^2H nmr Line Shapes

In Fig. 3 the ^2H nmr line shapes of the $-ND_3$ group in PPNCl are shown for five different temperatures. At 295 K, in the solid III phase, the quadrupolar splitting is 36 ± 1 kHz. This value is lower than the typical value of 41 kHz which one obtains for a N–^2H bond with a QCC of 165 kHz performing pure C_3 jumps. From the observed line shape one must conclude that additional motion is present in order to reduce the quadrupolar splitting. Additional evidence for this motion was also observed in the ^2H line shapes of variable echo delay experiments in the solid III temperature region of intermediate exchange. This temperature region was easily accessible since the ^2H relaxation of the $-ND_3$ groups is near its T_{1Z} minimum at room temperature (*vide infra*). The intermediate exchange line shapes could not be simulated with a QCC < 165 kHz and a pure C_3 jump model. Also, $^2H-^{14}N$ dipolar interactions [28] alone cannot explain the observed line shapes since this coupling will not give rise to an additional reduction of the quadrupolar splitting. However, this coupling could explain some of the features of the intermediate exchange line shapes of $-ND_3$ groups.

From the crystal structure of phenethylammonium chloride [1] it is known that the $-ND_3$ group rotates in an asymmetric potential. The symmetry of this potential can be minicked by a two site exchange process in addition to the C_3 jumps. We assume a similar process to be responsible for the ^2H nmr line

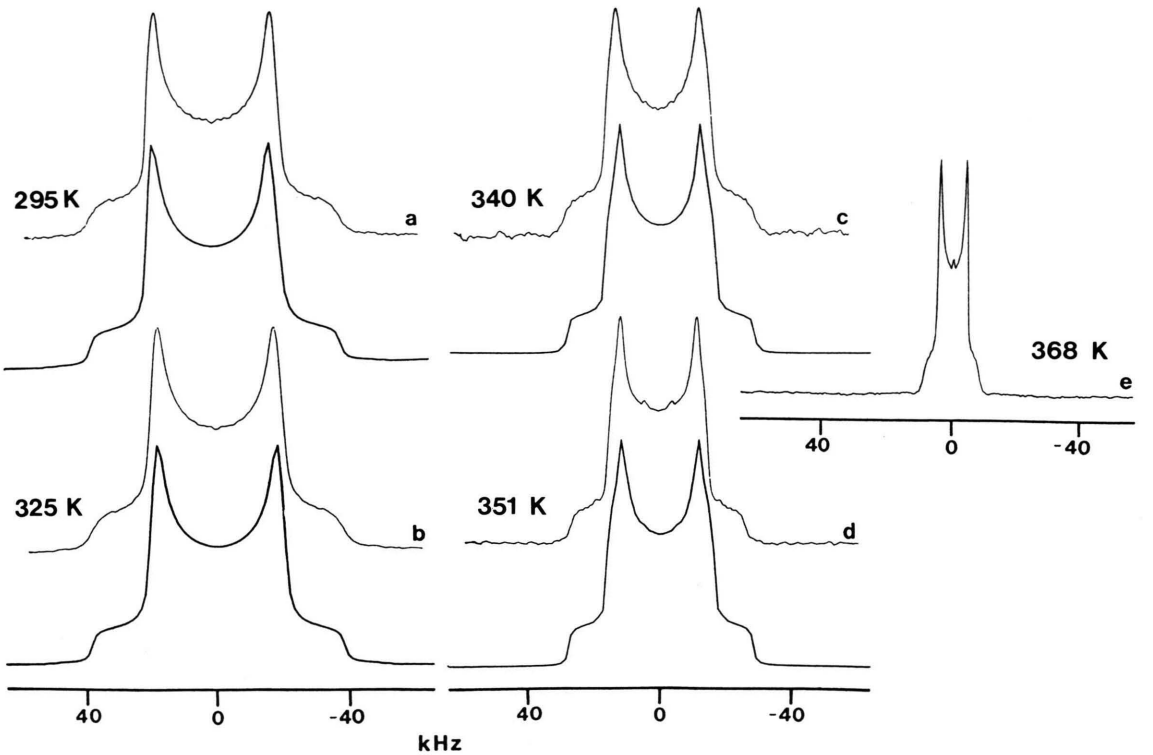

Fig. 3. ^{2}H nmr line shapes of the ND_3 group in PPNCl at (a) 295 K, (b) 325 K, (c) 340 K, (d) 351 K, (e) 368 K. All spectra were acquired with a 40 μs echo delay. The simulation parameters are: (a, b) QCC = 165 kHz, both R_3 and R_2 fast, $\beta_3 = 70.5°$ and $2\delta_2 = 24°$. For (c): $(QCC)_{effective} = 44$ kHz, this value includes the averaging over the C_3/two site exchange model, $2\delta_2' = 34°$ for the additional two site exchange, $\beta_3 = 70.5°$. And for (d): same as in (c) except for $2\delta_2' = 38°$. All averaging processes were taken in the fast motion limit and 40 μs echo delays were used. The simulation is always the lower spectrum of a set ot two and R_2 and R_3 refer to the two and three site exchange rates, respectively. A similar notation is used for the jump angles.

shape of the $-ND_3$ groups in the solid III phase of PPNCl. Using this model, Fig. 3a could be simulated. Since, at this temperature, both motions are fast compared to the QCC (=165 kHz), the line shape is not sensitive to the details of the model.

At 340 K, in solid II (Fig. 3c), the ^{2}H line shape is axially asymmetric. The observed asymmetry increases with increasing temperature until in solid I the line shape again becomes axially symmetric. The changes in line shape upon the solid III–solid II phase transition, is also paralleled by the observed changes in the ^{2}H spin-lattice relaxation times (*vide infra*). Upon the solid III–solid II transition, the ^{2}H spectra of the $-CD_2-$ groups also start to show spectral asymmetry (*vide infra*). This indicates that in solid II the C–N axis performs a low symmetry two-site exchange motion with an apparent temperature dependent jump angle (see Figs. 3c, d). The deuterium nmr line shapes of the $-C_6D_5$ group indicate that in solid II (*vide infra*) motion in addition to the phenyl ring C_2 flips is present. This additional motion reorients the $C_{para}-C_{ipso}$ axis in space over small angles. Thus in solid II, both ends of the phenylpropylammonium ion perform small-angle motions which are not directly related to molecular symmetry axes. From this it is clear that it will be difficult to determine, from ^{2}H line shapes alone, the exact cause of the observed averaging of the line shapes in solid II. However, one can exclude reorientational processes which assume one or both end(s) of the molecule to be fixed in space.

Here we will explain the observed asymmetric ^{2}H line shapes of the $-ND_3$ group with a simple two-site exchange model [17, 18, 29] incorporating equal populations. This model predicts the following relation

between the efg tensor components in principal axes and jump averaged frame:

$$V_{xx}^{J} = V_{zz} \sin^2 \delta + V_{xx} \cos^2 \delta\,, \tag{8a}$$

$$V_{yy}^{J} = V_{yy}\,, \tag{8b}$$

$$V_{zz}^{J} = V_{zz} \cos^2 \delta + V_{xx} \sin^2 \delta\,. \tag{8c}$$

The angle 2δ represents the jump angle between the sites and the index J refers to the jump averaged frame. Note that the z_J axis was chosen, such that it intersects the angle 2δ between the two sites and y_J was taken perpendicular to the plane made by the two sites. Equation (8 b) shows that the V_{yy} component of the efg tensor remains unchanged in the flip-averaged frame. Thus one will observe a constant value for V_{yy} independent of the jump angle. Using this model the ^{2}H nmr line shapes of the $-ND_3$ groups in the solid II phase could be simulated (see Figures 3 c, d). The application of the model is justified since the V_{yy} component of the efg tensor of deuterons in the $-ND_3$ groups does not change, within experimental error, with temperature while the spectral asymmetry does change. The jump angle is thus a function of temperature. Although more complicated models could result in similar line shapes, from the observation that V_{yy} is constant one can conclude that whatever the exact details of the motion, the molecular reorientation must be planar.

Recently, Jurga et al. [30] successfully interpreted the ^{2}H nmr line shapes of selectively deuterated n-decylammonium chloride as a function of temperature in its various layered phases using a general jump model. The application of their model is facilitated by a knowledge of the crystal symmetry and structure. Since the ^{2}H nmr line shapes for PPNCl exhibit many features in common whith those of n-decylammonium chloride, the model proposed by Jurga et al. could, in principle provide a good description for the phenpropylammonium cation dynamics in PPNCl. Unfortunately the crystal structure of PPNCl is unknown. Also, PPNCl has a much shorter alkyl chain (C_3) than that of n-decylammonium chloride (C_{10}) making a direct comparison between the two compounds difficult. The important feature of the PPNCl solid II ^{2}H line shapes is the temperature independence of the V_{yy} tensor component for both the ND_3 and $-CD_2-$ groups (see Section iii)). In the jump model of Jurga et al. the temperature dependence of jump site populations would be expected to result in an observed temperature dependence of V_{yy}. The ^{2}H nmr spin-lattice relaxation times of the ND_3 group shown an abrupt increase at the solid II–solid I phase transition. This increase in mobility suggests a structural phase transition, i.e., a change in the hydrogen bonding network. Within the framework of a structural phase transition, a temperature dependent jump angle as proposed here for the solid II phase of PPNCl, will be considered as a simple but plausible interpretation of the ^{2}H nmr line shapes; however, it is by no means a unique interpretation of the data.

In solid I the ^{2}H spectra of the $-ND_3$ groups are again axially symmetric, with a quadrupolar splitting of 8 ± 0.5 kHz. In this phase the $-CD_2-$ groups also show an axially symmetric line shape with a quadrupolar splitting of 44 ± 1 kHz (*vide infra*). These splittings indicate large-angle reorientation of the C···N axis. In section iii) of this paper it will be shown that the observed reduction in the quadrupolar splittings of the $-ND_3$ and $-CD_2-$ groups is likely to arise from rotational jumps around a molecular reorientation axis. The angle between the rotation axis and the C–N bond can be calculated using (2). An angle of 45° or 63° is obtained.

ii) Reorientational Dynamics of the $-ND_3$ Group Obtained from ^{2}H nmr Spin-Lattice Relaxation Times

Spin-lattice relaxation times of Zeeman- and quadrupolar order were measured as a function of temperature for the $-ND_3$ group in solid II and the solid III phases of PPNCl. The relaxation times were obtained at the "$\theta = 90°$" and $\theta = 0°$ orientations in the powder patterns. Due to insufficient excitation, resulting from the finite length of the applied pulses [23, 27], and the applied line broadening of 0.5 kHz, the edges of the spectra were not always accurately defined. This prompted us to measure the relaxation times in a window of $\theta = 0° - 5°$, an approximation which is adequate for our purposes.

The temperature dependence of the spin-lattice relaxation times for the $-ND_3$ group in PPNCl is shown in Figure 4, a, b. The observed temperature dependence enabled us to obtain a QCC for the N–^{2}H bond from the minima in T_{1Z} and T_{1Q}. In Table 5 the T_1 minima are listed together with the calculated QCC's. The QCC's were calculated using (3), assuming that only C_3 jumps cause spin-lattice relaxation. Although the spread in the calculated values of the QCC is small, it can be concluded that the QCC obtained from T_{1Z} measurements is smaller than that obtained

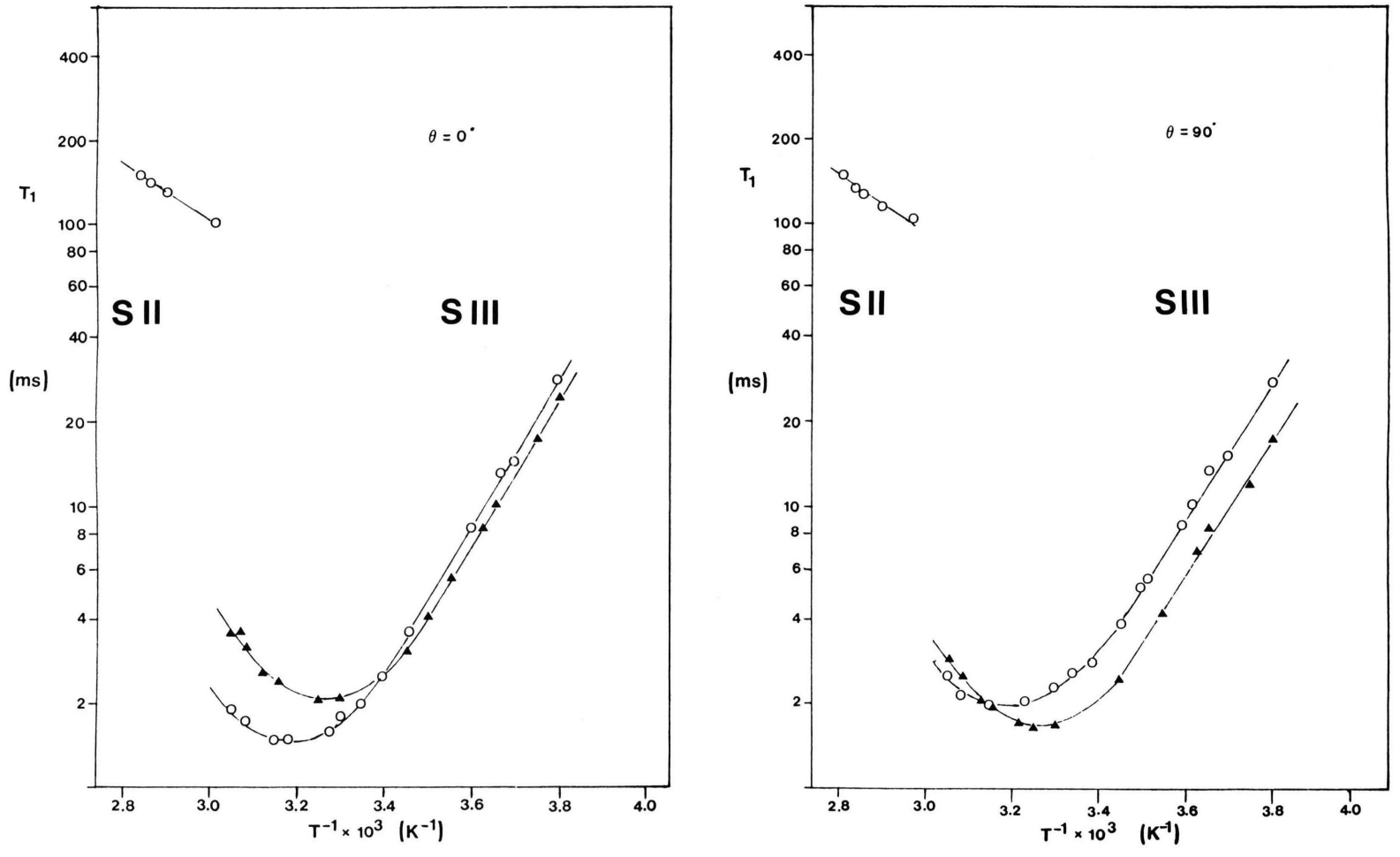

Fig. 4. ^2H Zeeman- and quadrupolar spin-lattice relaxation times for the $-ND_3$ group in PPNCl as a function of temperature. Triangles refer to quadrupolar order and the circles refer to Zeeman order.

Table 5. ^2H relaxation time minima and QCC's for PPNCl.

T_{1Z} (ms)			T_{1Q} (ms)	
$\theta = 0°$	"$\theta = 90°$"		$\theta = 0°$	"$\theta = 90°$"
1.5 ± 0.1	2.0 ± 0.1		2.1 ± 0.1	1.7 ± 0.1
		$\langle\chi^2\rangle^{1/2}$		
156 ± 5	164 ± 5		167 ± 5	173 ± 5

Table 6. Observed ratios of Zeeman- and quadrupolar spin-lattice relaxation rates for PPNCl $-ND_3$ ^2H relaxation.

$\theta = 0°$		"$\theta = 90°$"	
$\omega_0\tau \ll 1$	$\omega_0\tau \gg 1$	$\omega_0\tau \gg 1$	$\omega_0\tau \gg 1$
–	0.87 ± 0.07	–	0.63 ± 0.02

from T_{1Q} experiments. The origin of this could be the additional motion as discussed in the previous section. This additional motion gives rise to different spectral densities at ω_0 and $2\omega_0$ in the temperature region of the relaxation time minima. Similar observations were made for the relaxation of $-ND_3$ group in phenpropylammonium bromide [31].

At temperatures above the solid III–solid II phase transition in PPNCl, the ^2H relaxation times of the $-ND_3$ group increase by approximately two orders of magnitude. For the solid II phase, the "$\theta = 90°$" and the $\theta = 0°$ orientations of the powder pattern do not relax with the same rate, indicating that the reorientation mechanism still involves jumps instead of small-angle diffusion [32].

The observed ratios of the Zeeman- and quadrupolar spin-lattice relaxation rates are listed in Table 6. Comparing these with the calculated values from Table 4, one notes that C_3 jumps dominate the spin-lattice relaxation. This is consistent with the C_3/two site exchange model proposed in part i), since the two-site exchange model, if treated independently, results in low values of the spectral densities compared to that for the C_3 jumps. Using the theory outlined by Torchia and Szabo [19], it can be shown that the time correlation function $C_{a,a'}(t)$ for a combined C_3 jump and two-site exchange process can be written as [31]

$$C_{a,a'}(t) = \sum_{b=-2}^{2} |d^{(2)}_{0,b}(\Theta)|^2 \, \Gamma_{b,b}(t) \, d^{(2)}_{b,a}(\delta) \, d^{(2)}_{b,a'}(\delta) \, \Gamma_{a,a'}(t), \quad (9)$$

where Θ represents the angle between the $N-^2H$ bond and the C_3 jump axis and 2δ is the two site exchange angle. To reduce the mathematical complexity, only diagonal elements of the C_3 jump matrix included in the calculations. Thus $\Gamma_{b,b'}(t)$ was replaced by $\Gamma_{b,b'}(t)\,\delta_{b,b'}$ where $\delta_{b,b'}$ represents the Kronecker delta function. It was also assumed that the two sites occur with equal probability. For small values of δ it then follows that only those terms $C_{a,a'}(t)$, characteristic for C_3 jumps, dominate the relaxation of ^2H magnetization.

Experimental spectra of the $-ND_3$ group in the solid III phase of PPNCl can thus be simulated with a QCC of 165 ± 5 kHz. This value compares well with the QCC obtained by Oldfield et al. [21] for $-CD_3$ groups in some amino acids. Although they measured the T_{1Z} ("$\theta = 90°$") minimum (2.1 ± 0.3 ms) for one of the amino acids, they obtained the QCC from a 138 K rigid lattice spectrum. The activation energy E_a for the reorientation of the $-ND_3$ group in PPNCl is 47 ± 5 kJ mol^{-1} in the solid III phase.

iii) Reorientational Dynamics of the $-CD_2-$ Group

Deuterium nmr line shape studies of the $-CD_2-$ group in PPNCl as a function of temperature allow one to pobe the motion of the alkyl-chain or at least the $-CD_2-$ group adjacent to the ammonium head group. Reorientational motion affecting the ^2H nmr line shape of the $-CD_2$ group is also likely to be reflected in the ^2H nmr spectra of the ammonium head group. One exception is the motion around the $C_\beta-C_\gamma$ axis, where the index α indicates the C atom adjacent to the ammonium head group. Rotation around this axis will affect the $-CD_2-$ line shape but not that of the $-ND_3$ head group. In Figure 5, ^2H nmr line shapes of the $-CD_2-$ in PPNCl are shown for several temperatures.

For the solid III phase at 305 K, the ^2H nmr line shape (Fig. 5a) indicate small angle librational motion giving rise to a quadrupolar splitting of 108 ± 2 kHz. This splitting is smaller than the characteristic value of 120 kHz for a static aliphatic $C-^2H$ bond normally encountered [18, 33]. The spectrum obtained at 305 K could be simulated with a QCC of 165 kHz and a small libration angle; for simplicity, the QCC is taken similar to that observed in the ^2H nmr line shapes of the $-ND_3$ groups in solid III. A QCC of 165 kHz could be considered to be somewhat low for an aliphatic deuteron but is certainly not uncommon

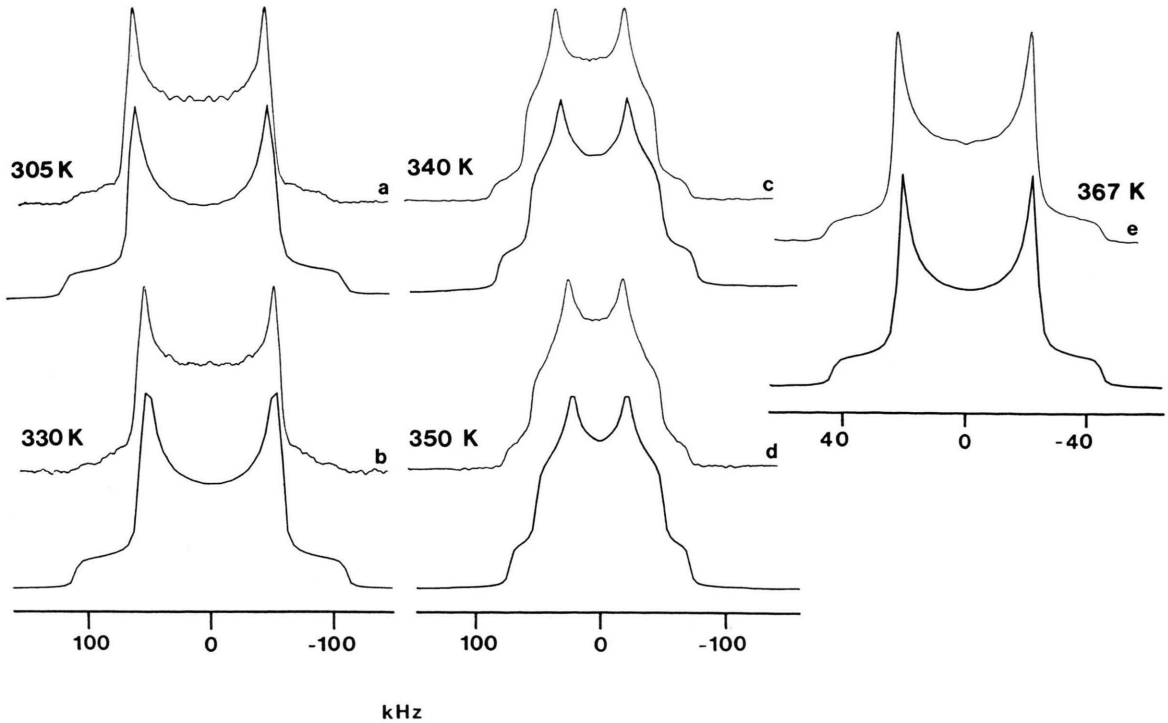

Fig. 5. ^{2}H nmr line shapes of the CD_2 group in PPNCl at (a) 305 K, (b) 330 K, (c) 340 K, (d) 350 K and (e) 367 K using a 40 μs echo delay. The simulation parameters are: (a) QCC = 165 kHz, fast R'_2, $2\delta'_2 = 24°$. (b) QCC = 160 kHz, R_2, fast and $2\delta'_2 = 24°$, indicating additional small angle isotropic averaging, reducing the QCC. (c) $(QCC)_{eff.} = 144$ kHz, $2\delta'_2 = 48°$ and R'_2 is fast. (d) $(QCC)_{eff.} = 142$ kHz, $2\delta'_2 = 52°$ and fast exchange. (e) QCC = 165 kHZ, $\beta'_3 = 72°$ and fast C_3 flips. The QCC values in (c) and (d) refer to the motionally averaged value obtained at 330 K.

[10a, 34]. Although difficult to determine due to the presence of line broadening arising from dipolar coupling to nearby ^{1}H nuclei, a small spectral asymmetry could be present in the line shape of Figure 5a. Low temperature (173 K) ^{2}H nmr measurements of the $-C_\alpha D_2-$ groups in the related salt, phenpropylammonium bromide, indicate an axially symmetric ^{2}H nmr line shape with a quadrupolar splitting of 122 kHz [31]. Upon heating of the sample the quadrupolar splitting narrows to 100 kHz at 341 K, although the sample is still in the same solid phase. This reduction is likely to be due to thermally activated small angle motions of the $-C_\alpha D_2-$ group. We assume a similar process to be responsible for the observed ^{2}H spectra of the $-CD_2-$ group in PPNCl.

At temperatures above 335 K, in solid II, the onset of large-amplitude, low-symmetry motion occurs. The rate at which this motion occurs is larger than the QCC since no changes in the overall ^{2}H nmr line shape was observed upon changing the solid echo delays (τ_1 and τ_2) from 40 μs to 160 μs. To confirm this, the Zeeman spin-lattice relaxation rates were measured at the V^J_{xx} position in the powder line shape for two temperatures. Some of the relaxation spectra obtained at 335 K are shown in Figure 6. The spectra clearly show the angular dependent relaxation of Zeeman order across the powder pattern. At 335 K, $T_{1Z}(V^J_{xx}) = 222 \pm 20$ ms and at 353 K, $T_{1Z}(V^J_{xx}) = 277 \pm 30$ ms, indicating that the reorientation is in the fast motion limit, i.e., $\omega_0\tau < 1$. The exact details of the motion are difficult to describe since there is more than one possible model giving rise to the same spectral features. Two plausible models are gauche-trans isomerization [34] and a simple two-site exchange [17, 18, 29]. However, these two models are expected to give rise to different temperatures dependencies of the ^{2}H nmr line shapes. With increasing temperatures one expects the population of the gauche isomers to increase. This will affect the ^{2}H nmr line shapes in such a way that the absolute value of the V_{yy} efg component of the powder pattern reduces with increasing temperature. For the two site exchange model one expects the

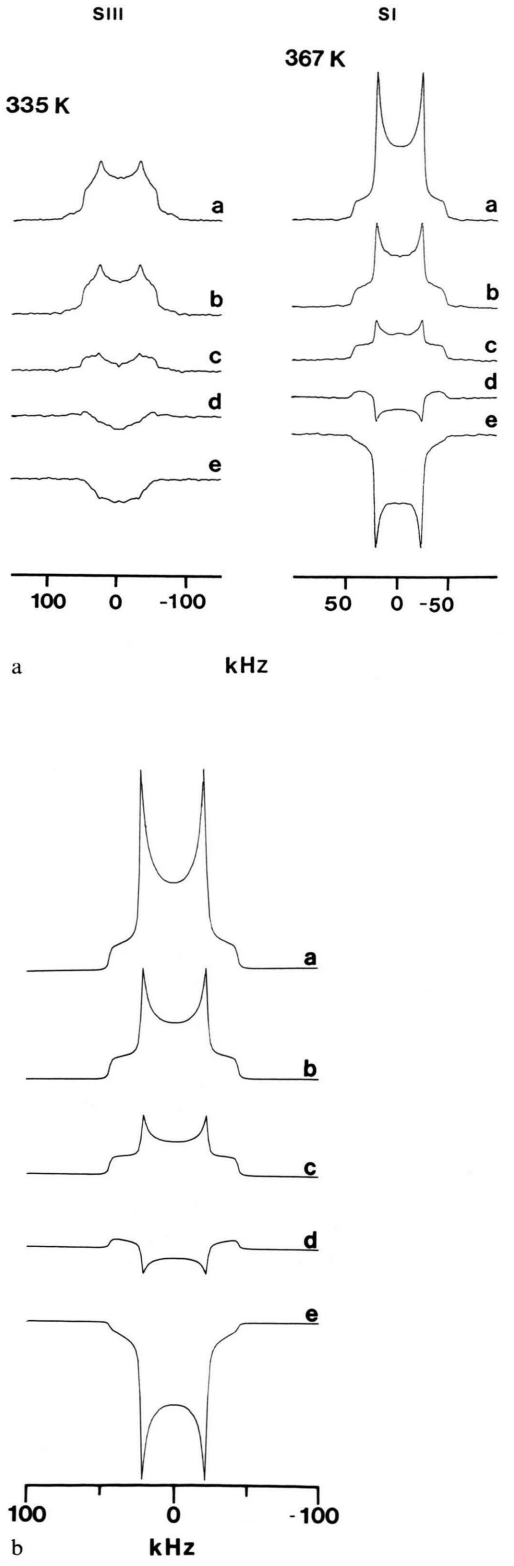

jump angle to increase with temperature, if allowed by the crystal structure [18]. As a result, the ^2H nmr line shape will change but, in contrast to the gauche-trans isomerization, the absolute value of the V_{yy} component will not change. Since the V_{yy} component of the $-CD_2-$ ^2H nmr line shape in PPNCl changes from $\pm(54\pm1)$ kHz at 305 K to $\pm(52\pm1)$ kHz at 350 K, we conclude that gauche-trans isomerization is not the dominant reorientation responsible for the observed line shapes in solid II. However, as pointed out by Smith et al. [17] and Griffin et al. [35], even a small population of the gauche isomer can reduce V_{yy}. The observed, small, reduction of V_{yy} in PPNCl could be accounted for by a small population of gauche bonds. In the line shape simulations this reduction will be introduced by using an effective QCC (see Figure 5). The two-site exchange angle 2δ is temperature dependent; $\delta=23°$ at 335 K, 24° at 340 K and 26° at 350 K. Comparing these angles with the ones obtained for the $-ND_3$ group in solid II, one observes that the two-site exchange is more restricted at the head group.

Figure 5e shows the ^2H line shape at 367 K. Here the motion narrows the quadrupolar splitting to 44 ± 1 kHz and results in an axially symmetric powder pattern. In Fig. 6a a Zeeman relaxation rate experiment at 367 K is shown for several values of the relaxation delay. Since the $-ND_3$ and $-CD_2-$ group are coupled through a bond, large amplitude motion affecting the ^2H nmr line shape of the $-CD_2-$ group is likely to affect the deuterium nmr spectrum of the $-ND_3$ group. One exception is the reorientation around the $C_\beta-C_\gamma$ bond which influences the $-CD_2-$ line shape but not that of the $-ND_3$ group. The observed additional reduction of the quadrupolar splitting in the ^2H nmr line shape of the $-ND_3$ group is not equal to that observed for the $-CD_2-$ group; 0.19 and 0.36 respectively. Thus, gauche-trans isomerization can not be an important reorientation mechanism since equal reduction factors are expected in the case

Fig. 6. a) ^2H Zeeman spin-lattice relaxation experiment on the CD_2 group of PPNCl in solid III at 335 K and in solid I at 367 K. The variable delays in the 335 K spectra are (from a to e): 8 s, 0.5 s, 0.2 s, 0.1 s and 5 ms. For the 367 K spectra (from a to e): 2 s, 0.3 s, 0.2 s, 0.1 s and 5 ms. The 335 K spectra are characteristic of two site exchange and the 367 K spectra are characteristic of C_3 jumps. The spectra were acquired with a 40 μs echo delay. b) Deuterium line shape simulation of the 367 K inversion recovery spectra shown in Figure 6a. Parameters used are $\beta_3=72°$, QCC = 165 kHz and $R_3=2.1\pm0.1\times10^{10}\ s^{-1}$.

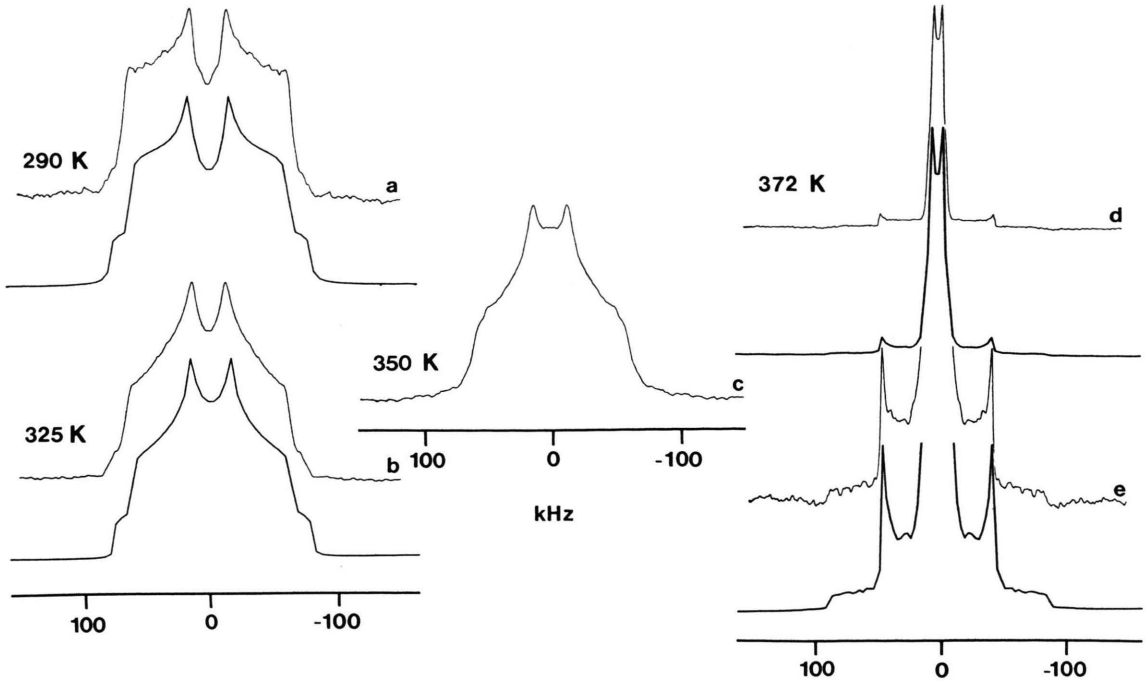

Fig. 7. ^{2}H nmr line shape of the C_6D_5 group in PPNCl at (a) 290 K, (b) 325 K, (c) 350 K and (d, e) 372 K. The simulation parameters are: (a) QCC = 170 ± 6 kHz, C_2 flips with $R_2 = 5 \times 10^6$ Hz. For (b) we used the same parameters as for (a) except, R_2 is fast. Spectrum (e) is an expansion of (d) and was simulated with: QCC = 170 kHz, rotational diffusion around the $C_{para}-C_{ipso}$ axis and superimposed on that a rotation around an axis making an average angle of 25° with the $C_{para}-C_{ipso}$ axis, introducing an extra reduction of 0.7 of the quadrupolar splittings.

of equally populated gauche and trans sites. If the sites are not equally populated spectral asymmetry should be observed. Also C_3 jumps around the $C_\alpha \cdots C_\beta$ axis can be excluded since this will give rise to an axially symmetric powder pattern for both groups but with a quadrupolar splitting of 40 ± 1 kHz for the $-CD_2-$ group and 13 ± 1 kHz for the $-ND_3$ group, assuming a QCC of 165 kHz as used in the interpretation of the solid III and solid II deuterium spectra.

Since the observed powder patterns of the $-ND_3$ and $-CD_2-$ groups are axially symmetric, molecular motion about a three- or higher-fold axis is present. In the solid I phase, the ^{2}H nmr spectra of the deuterium labelled phenyl ring of PPNCl indicate that in the addition to the diffusion around the $C_{para}-C_{ipso}$ axis, a rotation about an axis oriented slightly off with the $C_{para}-C_{ipso}$ axis (*vide infra*). Thus from the $-CD_2-$ ^{2}H nmr line shapes it may be concluded that the whole phenpropylammonium ion rotates around the same axis in solid I. Using (2), the angle between the rotation axis and the C–^{2}H bond and the C–N axis can be obtained. For the C–^{2}H bond an angle of 72° or 41° and for the C–N bond an angle of 45° or 63° is calculated. In the case of the $-CD_2-$ group, the angle between the rotation axis and the C–^{2}H bond can be determined from the Zeeman relaxation rate experiment of Figure 6a. From this figure it is clear that $T_{1Z}(\theta = 0) < T_{1Z}(\text{“}\theta = 90°\text{”})$. Assuming C_3 jumps around the proposed molecular axis, Eq. (4) shows that, due to the dependence of the spectral densities, changing Θ from 72° to 41° reverses the T_{1Z} anisotropy, i.e., $T_{1Z}(\text{“}\theta = 90°\text{”}) < T_{1Z}(\theta = 0°)$. Thus, using this model, the angle between the C–^{2}H bond and the rotation axis must be 72°. A simulation of the Zeeman relaxation rate experiment at 367 K is shown in Fig. 6b where a jump rate of $2.1 \pm 0.1 \times 10^{10}\,s^{-1}$ was obtained.

iv) Reorientational Dynamics of the $-C_6D_5$ Group

In Fig. 7 the ^{2}H nmr line shape of the phenyl-ring is shown for a few temperatures. In the solid III phase, the para deuteron resonance was saturated during data collection due to the relatively short recycle delay

employed. Note that even for C_2 jumps around the $C_{para}-C_{ipso}$ axis, the para deuteron is not being averaged by the motion and should give rise to a static powder pattern. For $C-^2H$ bond in phenyl-rings QCC's of 170–180 kHz (and $\eta=0$) have been reported by several researchers [11, 36–39]. The ^2H line shapes in solid III are characteristic for phenyl-rings performing C_2 flips around the $C_{para}-C_{ipso}$ axis with a jump angle $2\delta=120°$. At 290 K the C_2 flips are in the intermediate exchange region, allowing one to obtain a jump correlation time from the line shape. At 290 K a line shape simulation (see Fig. 7) results in a C_2 jump rate of $5.0 \pm 0.5 \times 10^6\ s^{-1}$. At 325 K the jumps are in the fast exchange limit.

In solid II, Fig. 7c, additional motion, which reorients the $C_{para}-C_{ipso}$ axis in space, takes place. The ^2H nmr line shape is difficult to interpret.

In solid I, at 372 K, a ^2H nmr line shape typical for rotational diffusion of a phenyl-ring around the $C_{para}-C_{ipso}$ axis [37, 38] was observed. However, if only small angle diffusion around the $C_{para}-C_{ipso}$ axis takes place, the ^2H nmr line shape should consist of an axially symmetric powder pattern with a quadrupolar splitting of 1/8 times that of a static spectrum and an integrated, normalized intensity of 4/5. Superimposed on that the line shape of the para deuteron with a quadrupolar splitting equal to that of a static deuteron and an integrated, normalized intensity of 1/5. The observed splitting of the inner doublet in Fig. 7d, e is less than that for pure rotational diffusion around the $C_{para}-C_{ipso}$ axis. Motion responsible for this also averages the efg of the para deuteron. The additional motion results in an additional reduction factor for the ^2H nmr line shape of 0.7. How this reduction factor is related to a rotation axis is difficult to visualize from molecular geometry. However, this additional motion can be described by the statement that the additional reorientation axis makes an angle of approximately 25° with the $C_{para}-C_{ipso}$ rotation axis, describing the effect as an average over all the phenyl deuterons. This is the first example that we are aware of where a substituted phenyl-ring appears to undergo rotational diffusion in the solid state.

V. Conclusions

In this paper the dynamics of the cation in phenpropylammonium chloride has been studied using ^2H nmr. Both line shape and relaxation studies were used in order to describe the dynamics of the $-ND_3$, $-CD_2-$ and $-C_6D_5$ groups. It was found that substantial molecular motion was present even in the low temperature phase, solid III.

In solid III the ^2H relaxation of the $-ND_3$ group could best be described by C_3 jumps, and from the relaxation time minima a QCC of 165 ± 5 kHz was obtained. This value of the QCC was used to simulate the ^2H line shapes, assuming additional, two-site exchange, motion to be present. Evidence for this additional motion was also inferred from variable echo delay experiments in the intermediate exchange region. The reorientation of the methylene group adjacent to the $-NH_3$ group is restricted to small-angle libration in the solid III phase. Deuterium line shape studies indicate that the librational angle increases with increasing temperature. In this phase the rings perform C_2 jumps around the $C_{para}-C_{ipso}$ axis. At 290 K the ring flips are in the intermediate exchange region (jump rate $=5.0 \pm 0.5 \times 10^6$ Hz), but at $T > 325$ K the jumps are in the fast motion limit.

In the solid II phase of PPNCl complicated overall motion was inferred from the ^2H nmr spectra. All three groups exhibited spectra indicative of motion in addition to that already present in solid III. The nature of this additional motion is such that it induces spectral asymmetry in the line shapes of the $-ND_3$ and $-CD_2-$ groups. Even the phenyl ring undergoes motion in addition to the $C_{para}-C_{ipso}$ ring flips, reorienting this axis over small angles in space. The exact origin of this motion could not be determined; also, there is some indication that the motions in the three groups are coupled to some extent. However, the ^2H nmr line shapes of the $-ND_3$ and $-CD_2-$ groups could be simulated using a simple two site exchange model since the ^2H line shapes indicate planar motions. Thus in solid II the alkyl chain of the phenpropylammonium ion undergoes large amplitude motion with a temperature dependent jump angle. The onset of this motion could trigger the solid III–solid II phase transition [3].

Finally in solid I, the ^2H nmr line shapes of all three groups indicate the presence of whole ion rotation. In this phase the phenyl-rings undergo rotational diffusion around the $C_{para}-C_{ipso}$ axis and, in addition, rotation around a molecular axis. The angle between the molecular axis and the $C_{para}-C_{ipso}$ axis is estimated to be 25°. Rotation around the molecular axis was also found to affect the ^2H line shape of the $-ND_3$ and $-CD_2-$ groups. From the observed reduc-

tion of the quadrupolar splittings, angles of the C–^{2}H bond and the C–N bond with the rotation axis could be determined. The observed values indicate that the alkyl chain is not likely to be in the all-trans conformation since there is no direct geometrical relation between the obtained angles and an all-trans conformation of the phenproylammonium ion. Using a T_{1Z} relaxation experiment, the rotation angle of the C–^{2}H bond was determined to be approximately 72°. This experiment also showed that C_3 jumps of the ion around the molecular axis do indeed provide a reasonable description of this reorientational process.

Acknowledgements

We would like to thank Professor M. A. White and Dr. M. van Oort for their interest in this work and for supplying us with deuterated samples of PPNCl. We thank Professor O. Knop and Professor K. R. Jeffrey for several helpful comments and a referee for bringing ref. [30] to our attention. Also, we wish to thank Professor R. G. Griffin, Professor R. J. Wittebort, and R. Weber for providing us with copies of the deuterium line shape simulation program described in [10b]. We are grateful to NSERC of Canada for financial support.

[1] G. Tsoucaris, Acta Cryst. **14,** 909 (1961).
[2] S. Roe, O. Knop, and T. S. Cameron, unpublished results.
[3] M. J. M. van Oort and M. A. White, Thermochim. Acta **139,** 205 (1989).
[4] M. L. H. Gruwel and R. E. Wasylishen, Z. Naturforsch. **46a,** 691 (1991).
[5] A. Abragam, Principles of Nuclear Magnetism, Oxford University Press, Oxford 1961.
[6a] H. W. Spiess and H. Sillescu, J. Magn. Reson. **42,** 381 (1981).
[6b] A. Vega and Z. Luz, J. Chem. Phys. **86,** 1803 (1987).
[7] J. H. Davis, K. R. Jeffrey, M. Bloom, M. I. Valic, and T. P. Higgs, Chem. Phys. Lett. **42,** 390 (1976).
[8] I. Solomon, Phys. Rev. **110,** 61 (1958).
[9] G. Bonera and M. Galimberti, Solid State Comm. **4,** 589 (1966).
[10a] K. Beshah, E. T. Olejniczak, and R. G. Griffin, J. Chem. Phys. **86,** 4730 (1987).
[10b] R. J. Wittebort, E. T. Olejniczak, and R. G. Griffin, J. Chem., Phys. **86,** 5411 (1987).
[11] D. M. Rice, R. J. Wittebort, R. G. Griffin, E. Meirovitch, E. R. Stimson, Y. C. Meinwald, J. H. Freed, and H. A. Scheraga, J. Amer. Chem. Soc. **103,** 7707 (1981).
[12] R. R. Vold and R. L. Vold, Adv. Magn. Optical Reson. **16,** 85 (1991).
[13] M. Mehring, Principles of High Resolution NMR in Solids, 2nd ed., Springer-Verlag, Berlin 1983.
[14] Y. Hiyama, J. V. Silverton, D. A. Torchia, J. T. Gerig, and S. J. Hammond, J. Amer. Chem. Soc. **108,** 2715 (1986).
[15] D. M. Rice, Y. C. Meinwald, H. A. Scheraga, and R. G. Griffin, J. Amer. Chem. Soc. **109,** 1636 (1987).
[16] S. W. Sparks, N. Budhu, P. E. Young, and D. A. Torchia, J. Amer. Chem. Soc. **110,** 3359 (1988).
[17] E. C. Kelusky, I. C. P. Smith, C. A. Elliger, and D. G. Cameron, J. Amer., Chem. Soc. **106,** 2267 (1984).
[18] M. G. Taylor, E. C. Kelusky, and I. C. P. Smith, H. L. Casal, and D. G. Cameron, J. Chem. Phys. **78,** 5108 (1983).
[19] D. A. Torchia and A. Szabo, J. Magn. Reson. **49,** 107 (1982).
[20a] H. W. Spiess, NMR, Basic Principles and Progress, Vol. 15 (P. Diehl, E. Fluck, and R. Kosfeld, eds.), Springer-Verlag, Berlin 1978.
[20b] H. W. Spiess, J. Chem. Phys. **72,** 6755 (1980).
[21] M. A. Keniry, A. Kintanar, R. L. Smith, H. S. Gutowsky, and E. Oldfield, Biochemistry **23,** 288 (1981).
[22] J. G. Powles and J. H. Strange, Proc. Phys. Soc. **82,** 6 (1962).
[23] D. J. Siminovitch and R. G. Griffin, J. Magn. Reson. **62,** 99 (1985).
[24] J. Jeener and P. Broekaert, Phys. Rev. **157,** 232 (1967).
[25] K. R. Jeffrey, T. C. Wong, and A. P. Tulloch, Mol. Phys. **52,** 307 (1984).
[26] M. J. M. van Oort, Ph.D. Thesis, Dalhousie University 1987.
[27] M. Bloom, J. H. Davis,. and M. I. Valic, Can. J. Phys. **58,** 1510 (1980).
[28] N. J. Heaton, R. R. Vold, and R. L. Vold, J. Chem. Phys. **91,** 56 (1989).
[29] S. K. Sarkar, P. E. Young, and D. A. Torchia, J. Amer. Chem. Soc. **108,** 6459 (1986).
[30] S. Jurga, V. Macho, B. Hüser, and H. W. Spiess, Z. Phys. B, Condensed Matter **84,** 43 (1991).
[31] M. L. H. Gruwel and R. E. Wasylishen, unpublished results.
[32] L. S. Batchelder, C. H. Niu, and D. A. Torchia, J. Amer. Chem. Soc. **105,** 2228 (1983).
[33] J. Seelig, Q. Rev. Biophys. **10,** 352 (1977).
[34] T H. Huang, R. P. Skarjune, R. J. Wittebort, R. G. Griffin, and E. Oldfield, J. Amer. Chem. Soc. **102,** 7377 (1980).
[35a] A. Blume, M. D. Rice, R. J. Wittebort, and R. J. Griffin, Biochem. **21,** 6220 (1982).
[35b] R. Ebelhäuser and H. W. Spiess, Ber. Bunsenges. Phys. Chem. **89,** 1208 (1985).
[36] C. R. Montgomery, N. J. Bunce, and K. R. Jeffrey, J. Phys. Chem. **92,** 3635 (1988).
[37] A. L. Cholli, J. J. Dumais, A. K. Engel, and L. W. Jelinski, Macromolecules **17,** 2399 (1984).
[38] R. A. Kinsey, A. Kintanar, and E. Oldfield, J. Biol. Chem. **256,** 9028 (1981).
[39] J. J. Dumais, L. W. Jelinski, M. E. Galvin, C. Dybowski, C. E. Brown, and P. Kovacic, Macromolecules **22,** 612 (1989).